Designing, prototyping, and testing an integrated e-axle for third-generation electric vehicles

Available online at www.sciencedirect.com

ScienceDirect

Transportation Research Procedia 72 (2023) 101–108

Transportation Research Procedia

www.elsevier.com/locate/procedia

Transport Research Arena (TRA) Conference

Designing, prototyping, and testing an integrated e-axle for third-generation electric vehicles

Michele De Gennaro[a]*, James H. Page[a], Tobias Wellerdieck[b], Antonio Lionetto[c], Sven Herber[d], Moritz Abbenhaus[d], Paolo Pescetto[e], Gianmario Pellegrino[e], Alfredo Primon[f], Patricio A. Torres[f], Andres Sierra-Gonzalez[g], Fernando Alvarez-Gonzalez[g], Michael Samsu Koroma[h], Daniele Costa[h]

[a]*Austrian Institute of Technology AIT GmbH, Giefinggasse 4, 1210 Vienna, Austria*
[b]*BRUSA Elektronik AG, Neudorf 14, 9466 Sennwald, Switzerland*
[c]*STMicroelectronics SRL, Stradale Primosole 50, 95121 Catania, Italy*
[d]*GKN Driveline Int. GmbH, Hauptstr. 130, 53797 Lohmar, Germany*
[e]*Politecnico di Torino, Department of Energy "Galileo Ferraris", 10129, Torino, Italy*
[f]*CRF, Centro Ricerche Fiat S.C.p.A., Orbassano, Italy*
[g]*Tecnalia, Basque Research and Technology Alliance (BRTA), 48160 Derio, Spain*
[h]*Mobility, Logistics and Automotive Research Centre, Department of Electric Engineering and Energy Technology, Vrije Universiteit Brussel, Pleinlaan 2, 1050 Brussels, Belgium*

Abstract

This paper presents the results of the H2020 project FITGEN, aiming at designing, prototyping, and delivering a functionally integrated e-axle ready for its implementation in third-generation electric vehicles. The manuscript concisely glances through the design results of all its main components, presenting the prototype delivered in April 2021. Preliminary performance results show that the e-motor is capable of 23,000 rpm, 130 kW continuous, 220 kW peak power and 210 Nm peak torque. The e-motor delivers up to 5.2 kW/kg, while the inverter delivers up to 35 kW/l. Its high-speed design allows for achieving these targets with 1.35 kg of rare-earth magnets, reducing by one-third the content of rare-earths against the best-in-class market available e-motor technology in 2022. The final FITGEN performance results and demonstration are expected to be delivered in the second semester of 2022.

Keywords: e-motor; inverter; e-axle; third-generation electric vehicles; FITGEN.

* Corresponding author. Tel.: +43-664-2351888; fax: +43-50550-6249, +43-50550-6595.
E-mail addresses: michele.degennaro@ait.ac.at; michele.degennaro.phd@gmail.com.

10.1016/j.trpro.2023.11.382

1. Introduction

The urgency of deep decarbonizing our economies and lifestyles and the transition to a circular economy has never been greater. To face these challenges, the European Union (EU) approved the European Green Deal Action Plan in December 2019. This plan has the ambition of transforming the EU into a modern, resource-efficient, competitive, and inclusive economy, ultimately decoupling economic growth from the use of resources, and achieving carbon neutrality in all economic sectors by 2050. In this framework, the decarbonization of transport plays a key role. Accounting for approximately one-fourth of the greenhouse gases emissions in the EU, it is a sector that calls for a massive shift to electrification to achieve carbon neutrality in the next three decades. In road transport, light duty vehicles are already on their way to electrification, with the record figure of 3.2 million new xEVs (PHEV and BEV combined) registered worldwide in the calendar year 2020, bringing the total count of circulating xEVs above 10 million vehicles by December 2020. Despite the pandemic, the market accelerated, pushing the sales figures of xEVs well beyond 5 million vehicles in 2021. More importantly, the European market is responding positively to this new class of vehicles, with new registrations of xEVs outnumbering diesel vehicles for the first time at the end of 2021. In this framework, the current technical challenge is not demonstrating technologies for electrification, but improving their performance while cutting their production cost, to make electric vehicles price-competitive against combustion vehicles. In fact, it is through enhanced affordability that xEVs will increase their user acceptance and market penetration, allowing the technology to deploy its carbon reduction potential at scale.

The European Commission has been massively investing in technologies for the electrification of transport for the last 15 years. The Green Car programme in FP7, the Green Vehicle programme in H2020 and, presently, the Cluster 5, Destination 5 in Horizon Europe have delivered a vast portfolio of electric technologies, encompassing xEVs' body frame, auxiliaries, power conversion and traction systems. This paper concerns the latter, presenting the nearly conclusive results of the H2020 project FITGEN (Functionally Integrated E-axle Ready for Mass Market Third Generation Electric Vehicles), granted under the topic LC-GV-01-2018 (EU Commission CORDIS, 2022). With its 5.8 million € budget and 5.0 million € funding, FITGEN aims to develop a functionally integrated e-axle ready for implementation in the third-generation electric vehicles (i.e., 2025 and beyond). The e-axle comprises a 6-phase Buried-Permanent-Magnet Synchronous Machine (later referred to as e-motor), a SiC-inverter (Silicon-Carbide) and a single-speed transmission. It is complemented by a DC/DC-converter for high voltage operation, fast battery charging, and an integrated AC/DC On-Board Charger (OBC).

The project consortium includes 8 partners and targets TRL7 by 2022, encompassing the demonstration of the e-axle on a FIAT 500-electric A-segment reference platform. FITGEN adopts as baseline the best-in-class market available technology in the reference year 2018, targeting the following progress beyond the state-of-the-art: (i) increase of 40% of the e-motor power density to 5.0 kW/kg at 20,000 rpm with a peak efficiency equal or above 96.5%, (ii) increase of 50% SiC-inverter power density to 25 kW/l with a peak efficiency of approximately 98-99%, (iii) affordable and integrated fast charge capability of 80 kW-average, and (iv) production cost equal or below 2,000 €/unit (cost of e-motor, power electronics and transmission, 2030 projection).

2. E-axle design results

2.1. Preliminary design

The FITGEN e-axle is natively designed to equip multiple vehicle platforms and brands. Three vehicle platforms have been adopted for its preliminary sizing: (1) the A-segment Battery Electric Vehicle (BEV) demonstrator in 2WD configuration (selected for the e-axle physical demonstration), (2) a small Sport Utility Vehicle (SUV) in Plug-in Hybrid Electric Vehicle (PHEV) 4-Wheel Driving (4WD) configuration with the combustion engine on the front axle and the electric traction on the rear axle, and (3) a large SUV BEV in 4WD configuration with the electric traction on both the front and rear axles. The main design and performance specifications are listed in Table 1. A set of speed profiles, i.e., the Worldwide harmonized Light vehicles Test Procedure (WLTP), the US06 type approval, a set of urban and mixed real driving cycles, and constant 110 km/h drive condition, have been adopted, targeting an electric driving range from the full battery with three charging stops greater than 700 km. Based on these, the electric motor

was sized for a single-speed transmission at a reduction ratio of 1:12.5, compatible with the operation of the e-motor equal to or above 20,000 rpm.

Table 1. Vehicle specifications (rows 1 – 5) and performance (rows 6 – 9).

Parameters	Unit	A-segment	Small SUV	Large SUV
Tyre rolling radius	m	0.3	0.32	0.34
Vehicle mass	kg	1,400	1,700	2,400
Rolling resistance	-	0.007	0.008	0.008
Product of drag coefficient and frontal area	m^2	0.75	0.9	0.85
Average 12V auxiliary power	W	300	500	700
Maximum speed	km/h	160	130	220
Acceleration time 0-100 km/h	s	10	12	7
Maximum gradient for 0.05g acceleration 0-10 km/h	%	30	30	45
Maximum gradient at a constant 100 km/h	%	5	5	5

A virtual integration study of the e-axle with the demonstrator A-segment vehicle platform has been carried out, encompassing five integration architectures, including both front and rear axle. This study assessed complexity, integration level, feasibility to achieve project targets and mechanical interference of the traction systems with other components (e.g., body frame, suspensions etc.). Fig. 1 shows the selected rear-axle driven integration architecture. The inverter, e-motor and transmission are integrated as a mono-block, with the DC/DC converter just above to minimize the length of the cables. The e-axle is mounted in rear wheel driving configuration on the vehicle prototype chassis, using the space in the boot and with a mechanical modification to the rear suspension system.

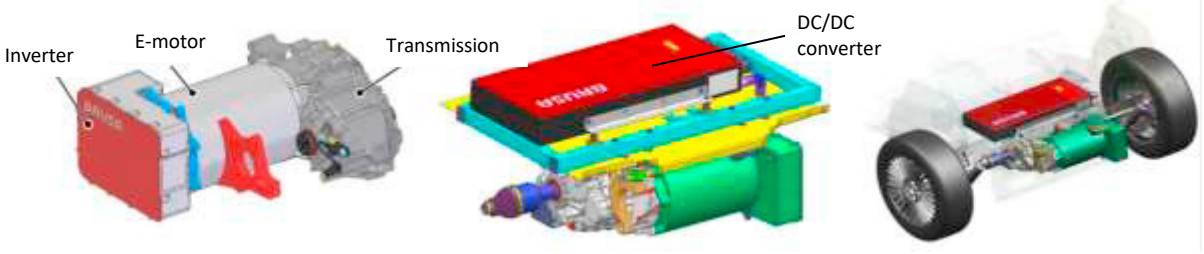

Fig. 1. FITGEN inverter-e-motor-transmission mono-block (left), mono-block with DC/DC converter (centre) and e-axle mounted in A-segment rear-wheel driving configuration.

2.2. E-motor design

The e-motor requirements for peak and continuous torque versus speed were derived from the target vehicle performance in Table 1, the transmission specification, and the project objectives. These include an e-motor power density above 5.0 kW/kg, a rotational speed above 20,000 rpm, and a peak efficiency above 96.5%. The design focused on three aspects: rotor and magnet geometry, stator winding, and housing geometry.

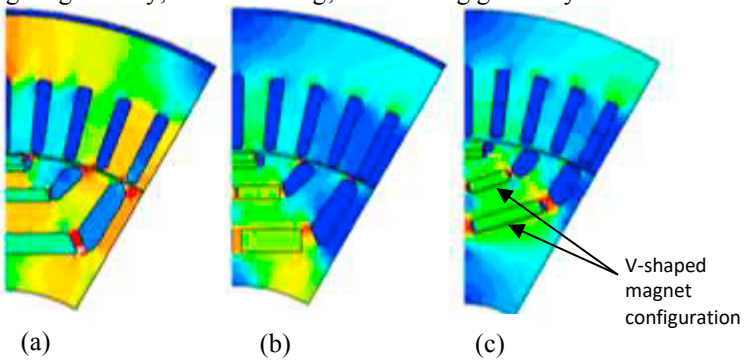

Fig. 2. Schematic view of the rotor and stator during rotor design optimization. a) First design; b) second design; c) third design.

The electric steel rotor was based on a proprietary design with three layers of permanent magnets and flux barriers (Zhou, et al., 2018). The design was further optimized for high rotational speed mechanical integrity and magnetic flux density. Fig. 2 shows the e-motor cross-sections, with six-phases and three-pole pairs, with rotor design optimization progressing from left to right. The blue to red color map represents low to high magnetic flux density. The first design (a) featured horizontal magnets and excessive mechanical between the cavities. The second design (b) featured split horizontal magnets and acceptable mechanical stress. The third design (c) featured V-shaped magnets, acceptable mechanical stress, and improved magnetic flux density. The resulting shaping of the magnetic flux density in the air gaps reduces losses in the electric steel.

The stator uses an innovative winding scheme using Formed-Litz Wire (FLW), which is suitable for automated production and has a high fill-factor, leading to low ohmic resistance at low-frequency AC, and good heat transfer for cooling. However, its main advantage over rival technologies is low ohmic resistance at high-frequency AC. This was demonstrated by a recent study comparing FLW with two common windings, pull-in winding (PIW) and hair-pin winding (HPW) (Dimier, et al., 2020). Fig. 3 reproduces from this reference schematic cross-sections of the three winding types and their respective variations in resistance with frequency. An innovative proprietary winding scheme has solved the relative inferiority of FLW in terms of turns number flexibility. Therefore, FLW offers overall far superior performance. In addition to utilizing these design advances, the project saw significant manufacturing advances, paving a clearer path to the series production of this and similar e-motors.

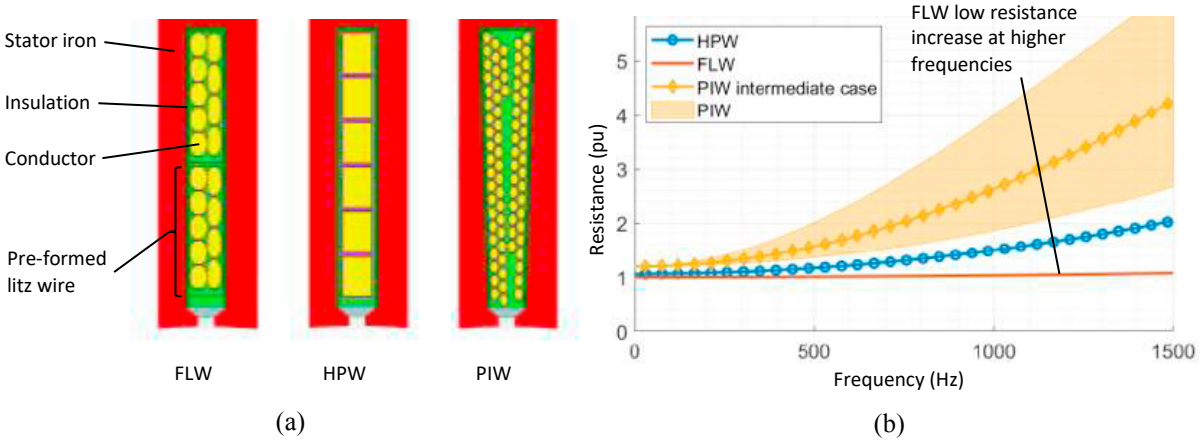

Fig. 3. a) Schematic view of a stator slot with FLW, HPW and PIW; b) variation of resistance with frequency of FLW, HPW and PIW.

The detailed design was carried out using an integrated workflow to optimize electromagnetic, thermal, and mechanical aspects of the e-motor. The e-motor and inverter are integrated into a single housing, reducing the total mass of the two components, while simplifying the cooling system and the electrical interfaces. This, along with the rotor and winding designs, the e-motor achieves 97.4% peak efficiency at approximately 170 Wh losses (e-motor only) for the type-approval WPLT cycle.

2.3. SiC–inverter design

A hard switching six-phase inverter using silicon carbide (SiC) power metal-oxide-semiconductor field-effect transistors (MOSFETs) was designed, comprising two sub-inverters each with three phases to drive the six-phase motor. Each sub-inverter drives one of the three-phase systems of the machine and consists of three half bridges and a DC-link capacitor. The topology allows a reduced power mode in case of a fault in one of the three-phase systems. Fig. 4 shows the power board of the inverter prototype. Various configurations of the board with discrete packages and integrated modules (delivering various outputs in power size, bounding and form factor) were analyzed. Characterization tests of the power semiconductors using double-pulse test-boards were carried out to complement the datasheet values and, thus, ensure that the design satisfies performance requirements. A discrete solution was

selected to facilitate greater flexibility to satisfy geometric constraints than power module solutions which offer higher power density but larger dimensions. Two MOSFETs, SCTW100N65G2AG through-hole technology (THT) and SCTH100N65G2-7AG surface mounted device (SMD), were investigated for switching losses. Using the software PLEX PLIMS and SPICE, their behaviour was simulated, and the optimal number of parallel MOSFETs per half-bridge was determined. While the conduction losses are the same due to the same on-state resistance, large differences were discovered when calculating the switching losses. The large parasitic inductances and the absence of a Kelvin source in the THT severely limit the switching speed at high drain currents. This resulted in the selection of the SMD. Four devices were parallelized for each power switch on the inverter power stage. In total, the inverter has 48 power devices.

Fig. 4. a) Prototype inverter with power stage on top and cooling fixture below; b) prototype inverter in integrated inverter-e-motor housing.

2.4. Transmission Design

The transmission was designed based on an existing highly efficient single-gear high-speed transmission. An existing load cycle from a representative FIAT BEV was scaled, to the project gear ratio, performance, and lifetime requirements, for the gearbox layout calculation. Investigations of the gear and bearing concept were then conducted to verify robust performance over the expected lifetime. The gearbox housing was modified to enable the interface with the e-motor, and three-dimensional mechanical stress simulations were performed to ensure mechanical integrity. With the operating temperature varying between -40°C and +140°C, the high efficiency of the gearbox means passive combined lubrication and cooling system was found to be sufficient. This reduced the weight and cost, because of the lack of a pump and corresponding control system. A temperature sensor in the gearbox allows mitigating measures to be taken in case of abnormal oil temperature. The transmission satisfies the maximum speed e-motor requirement for high-speed, and the final product is visible below as part of the e-axle in Fig. 7-(right).

2.5. Cooling System Design

The ability to keep the maximum temperatures of the e-motor winding insulation and magnets within acceptable limits over the whole operating range is essential to maintaining the performance and integrity of the machine. A three-dimensional computational model of the fluid dynamics and heat transfer in the e-motor, based on the Reynolds-averaged Navier-Stokes (RANS) equations with the k-omega SST turbulence model and energy equation, was developed, with mesh sizes of up to 120 million cells. Using this model, a coolant labyrinth within the e-motor housing was designed within the prescribed geometric constraints, a maximum overall pressure drop of 17 kPa, and a volumetric flow rate of 8 liters/min. Three variants of the model were used to design the system. The first variant comprised only the fluid domain of the liquid cooling system for the initial design. The second variant comprised the full e-motor geometry for calculating heat flux, heat transfer coefficient and temperature boundary conditions for the reduced geometry in the third variant. The third variant comprised only the stator iron, winding, potting, bearing plate, external housing, and liquid cooling system. This was used to carry out the design optimization and sensitivity studies.

The first variant design phase assessed the flow distributions of multiple labyrinth configurations, leading to selecting of the configuration apparent in Fig. 5-(a) and the number of circumferential channels set to deliver the target pressure drop at the prescribed flow rate. The configuration satisfied geometric constraints placed on the inlet and

outlet locations, rib shape and the requirements for gaps between the ribs and outer housing. Fig. 5-(a) highlights the initial flow along the axial channel into the first circumferential channel, which distributes coolant around the right-hand end of the annulus. The two flow paths to the outlet via the circumferential channels and the rib-outer housing gap are also highlighted. The third variant optimization and sensitivity phase saw the optimization of the required rib-outer housing gap size for minimal maximum winding temperature while verifying the insensitivity of the overall pressure drop to gap manufacturing variation. It also investigated the sensitivity of the pressure drop to rib width variation, informing the manufacturing process. Complete information can be found in (Page, et al., 2021).

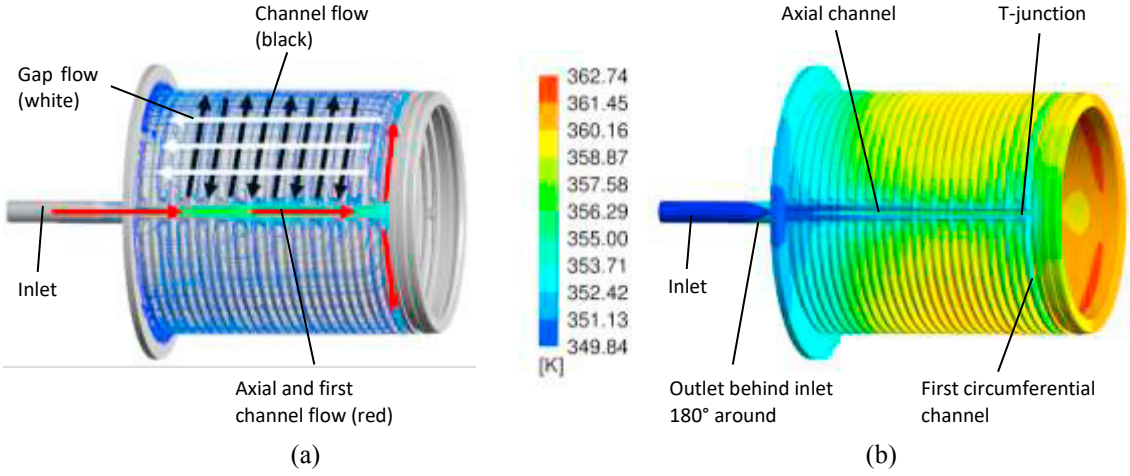

Fig. 5. Liquid cooling system design results: (a) flow field, (b) temperature field.

2.6. Control Design

A control system for the e-motor was developed.

Fig. 6 shows the block diagram, which can be viewed in three stages. The first stage considers the required torque, e-axle stator voltage, rotor speed, and outputs the optimal electric current set-points. These are found by using look-up tables, compiled using a high-fidelity mathematical model to represent the complex non-linear, coupled behaviour of e-motor. The second stage comprises the DC voltage active balancing system, necessitated by the cascaded topology of the 6-phase SiC-inverter, which balances the input voltages for the sub-inverters.

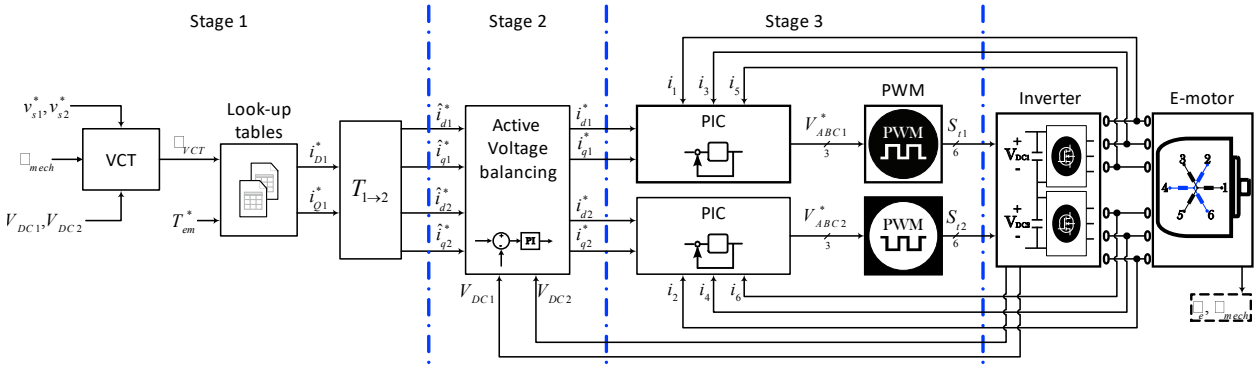

Fig. 6. Block diagram of the torque control implemented.

The third stage contains synchronous current regulation via Proportional-Integral Controllers (PICs) featuring feed-forward decoupling and anti-windup, and interleaved Pulse-Width Modulation (PWM) blocks which synthesize the

firing pulses for each sub-inverter (Sierra-Gonzalez, et al., 2021). In addition to exercising control, the system optimizes e-axle efficiency by adopting a variable DC-link strategy to dynamically adapt the inverter bus voltage based on the e-motor operating point. The DC-link variation is enabled by the high-performance DC/DC converter located between the battery and the 6-phase inverter. A custom control strategy minimizes the DC-link voltage without affecting control dynamics and minimizes switching losses in the inverter and the DC/DC converter (Pescetto, et al., 2021).

2.7. On-Board Battery Charger

A dedicated on-board battery charger (OBC) is a critical component of an EV, enabling low (3 to 6 kW) and medium (up to 11 kW) power charging for single- and three-phase main inlet, respectively. Standalone OBCs use a dedicated converter separate from the e-axle to charge the battery. Integrated OBCs achieve greater compactness by utilizing the inverter and e-motor as components. In FITGEN, a standalone OBC was developed and implemented, comprising two power conversion stages, a unidirectional three-phase T-type converter acting as an active front-end PFC rectifier, and a resonant LLC converter acting as an isolation DC/DC converter. The former uses three-level power conversion delivering good performance versus cost; the latter provides galvanic isolation between the AC grid and vehicle battery and delivers high efficiency by utilizing zero voltage switching. Preliminary sizing of the components was carried out and refined via detailed simulations using the software PLECS and SPICE, optimizing for volume, weight, and efficiency. A control strategy was designed and implemented. In addition to the standalone OBC, three integrated OBCs were designed: an isolated fully integrated (IFI) OBC, a non-isolated fully integrated (NIFI) OBC and an isolated semi-integrated (ISI) OBC. The IFI OBC uses the e-motor as an isolation transformer and the inverter for charge control. The NIFI OBC is an alternative solution utilizing e-motor leakage inductance. However, it does not provide galvanic isolation between the grid and battery during charging. The ISI OBC provides another alternative integrated solution utilizing the e-motor as an isolation transformer, this time excited by a controlled high-frequency signal with the disadvantage of requiring extra hardware.

3. E-axle performance results

In April 2021, the different parts and components of the e-axle were prototyped and assembled in multiple specimens, as depicted in Fig. 7.

Fig. 7. Assembled and integrated prototype inverter and e-motor (left) and inverter, e-motor, and transmission (right).

The stand-alone e-axle went through an extensive test campaign at various levels of integration during the second semester of 2021 and the first semester of 2022, during which the control algorithm was fine-tuned for best stability, maximum efficiency, and fail-safe operation. The consolidated set of bench results exhibit maximum rotational speed of 23,000 rpm (sustained overspeed at 27,600 rpm as per IEC 60034), maximum continuous power up to 130 kW, and peak power and torque up to 220 kW and 210 Nm, respectively. The FITGEN e-motor can deliver up to 5.2 kW/kg (active plus passive parts, +50% compared to the baseline 2018, increasing to 7.6 kW/kg considering active part only), while the inverter delivers up to 35 kW/l (+100% compared to the baseline 2018). Both exceed the project targets reported in section 1. Moreover, the high-speed design of the e-axle allows for achieving this performance by using

only 1.35 kg of rare-earth magnets (at 4.5 wt% Dy, 0.75 wt% Tb). This constitutes a breakthrough and a reduction of approximately one-third of Dy and Tb compared to the best-in-class e-motor technology in 2022, contributing to both reducing the environmental impact and the cost of the e-axle.

Lastly, the performance results have been complemented with a cradle-to-grave Life Cycle Assessment (LCA) based on the ISO 14040 and 14044. The functional unit was defined as a kilometer driven by a European B-segment BEV over its lifespan of 200,000 km for 12 years (ACEA, 2022) (Weymar & Finkbeiner, 2016). The LCA encompasses production, operation, and end-of-life, according to the method IPCC 2013 GWP 100y (IPCC, 2014). To compile the life cycle inventory, foreground data has been derived from the project and background data from the ecoinvent v3.6 database (Wernet, et al., 2016). The results show the FITGEN impact on climate change to be 27% lower than the 2018 baseline powertrain, mainly due to its superior energy efficiency. Instead, the production phase climate change impact is 2% lower than the 2018 baseline due to the reduced use of electronics, resulting from the increased integration of the e-axle parts. The final FITGEN test performance results (including LCA) and its integration on the demonstrator vehicle FIAT 500e will be delivered during the second semester of 2022.

4. Conclusions

This paper presents the results of the H2020 project FITGEN, as of May 2022, i.e., four months before the conclusion of its activities (planned for September 2022). Hence, despite not being final, the presented data provide a comprehensive overview of the project's achievements, focusing on the design of the e-axle components (e-motor, inverter, and transmission), cooling system, control, and the integrated charger. The performance of the e-axle measured at the test bench exhibit substantial improvements compared to the 2018 baseline, in line with the project's objectives. Moreover, the adoption of the FITGEN high-speed design has made possible a substantial reduction of the mass of the magnets in the rotor, resulting in a reduced amount of Dy and Tb compared to the best-in-class e-motor technology in the year 2022, with an inherent environmental benefit. From June to September 2022, the FITGEN e-axle is mounted and demonstrated on a FIAT 500e vehicle, whose performance will be assessed against the duty cycles described in Section 0. This vehicle will also function as a demonstrator for future exhibitions, supporting the industry to take over the technologies developed in FITGEN.

Acknowledgements

The authors are grateful to the European Commission for supporting the present work, performed within the EU H2020 project FITGEN (Grant Agreement 824335).

References

ACEA, 2022. *Vehicles in Use Europe 2022,* 2022: ACEA.

Dimier, T., Cossale, M. & Wellerdieck, T., 2020. *Comparison of Stator Winding Technologies for High-Speed Motors in Electric Propulsion Systems.* Gothenburg, Sweden , IEEE.

EU Commission CORDIS, 2022. *Functionally Integrated E-axle Ready for Mass Market Third GENeration Electric Vehicles.* [Online] Available at: https://cordis.europa.eu/project/rcn/218519/factsheet/en

Page, J. H. et al., 2021. *Three-Dimensional Design and Optimization of the Liquid Cooling System for the FITGEN E-Axle.* Detroit (US), SAE.

Pescetto, P., Sierra-Gonzalez, A., Trancho, E. & Pellegrino, G., 2021. *Variable DC-link Control Strategy for Maximum Efficiency of Traction Motor Drives.* Vancouver, ECCE-IEEE.

Sierra-Gonzalez, A. et al., 2021. *Control of dual three-phase IPMSM drive with cascaded DC-link capacitors for third generation EV.* Vancouver, ECCE-IEEE.

Wernet, G. et al., 2016. The Ecoinvent Database Version 3 (Part I): Overview and Methodology. *Int. J. Life Cycle Assess.,* pp. 1218-1230.

Weymar, E. & Finkbeiner, M., 2016. Statistical analysis of empirical lifetime mileage data for automotive LCA. *Int. J. Life Cycle Assess.,* Volume 21, pp. 215-223.

Zhou, T., Oeschger, D., Teufel, R. & Muntean, A., 2018. *Rotor for a synchronous drive motor.* EU, Patent No. Patent EP3651316A1.